



CHORUS

This is the accepted manuscript made available via CHORUS. The article has been published as:

Depletion-Induced Structure and Dynamics in Bimodal Colloidal Suspensions

M. Sikorski, A. R. Sandy, and S. Narayanan

Phys. Rev. Lett. **106**, 188301 — Published 3 May 2011

DOI: [10.1103/PhysRevLett.106.188301](https://doi.org/10.1103/PhysRevLett.106.188301)

Depletion-induced structure and dynamics in bimodal colloidal suspensions

M. Sikorski, A.R. Sandy, and S. Narayanan*

Advanced Photon Source, Argonne National Laboratory, Argonne, IL 60439, USA

Abstract

Combined SAXS and XPCS studies of moderately concentrated bimodal hard sphere colloidal suspensions in the fluid phase show that depletion induced demixing introduces spatially heterogeneous dynamics with two distinct time scales. The adhesive nature, as well as the mobility of the large particles is determined by the level of interaction within the monomodal domains. This interaction is driven by osmotic forces, which are governed by the relative concentration of the constituents.

PACS numbers: 82.70.Dd, 64.75.Xc, 61.05.cf

*Corresponding Author E-mail: sureshn@aps.anl.gov

Bimodal mixtures are found throughout nature in settings as diverse as volcanic ash deposits [1] and biological fluids such as blood and skimmed milk [2]. Industrially, such mixtures are useful as slurries or in suspension processing because their bimodal nature allows for enhanced packing or a mechanism to tune the viscosity of a fluid. Despite their ubiquity and usefulness, there remain many unanswered questions about the microscopic structure and dynamics of such materials and the connection of these microscopic properties to macroscopic properties like the viscosity. A distinguishing feature of bimodal systems is the complex relationship between their composition and properties. Their equilibrium structure is a non-trivial function of the size ratio of the constituent particles, $\kappa \equiv R_B/R_S$, where R_B and R_S are the radii of the larger and smaller particles, respectively, the total volume fraction ϕ of the particles, the relative concentration of the small (ϕ_S) and large (ϕ_B) species, $\varepsilon_B = \phi_B/(\phi_S + \phi_B)$, and the types of interaction between the constituents [3–6]. Mirroring their complex structure, the dynamics in such mixtures is also expected to be determined by the composition in a complex manner differing significantly from monomodal systems. Due to the relatively simple interactions between the particles, bimodal suspensions of hard spheres are extensively studied model systems. Experimentally, a major fraction of the work on bimodal colloidal suspensions has been devoted to understanding the link between the composition and structure [7–9]. There is considerably less knowledge about the impact of ε_B and ϕ on the dynamics. Most of the limited dynamics studies have focused on one class of colloidal suspensions, namely gels, and have revealed that the temporal and spatial dynamical heterogeneity, along with the α -relaxation in such systems are significantly altered when a minor fraction of small spheres is introduced into the host matrix of large spheres [10, 11]. Studies of colloidal gels have advanced our understanding of the relaxation processes in bimodal systems but the link between the composition and equilibrium dynamics in bimodal colloidal suspensions is still an open question. The aim of our work was to determine to what extent the dynamics in ergodic systems is affected by the large mismatch in the size of the constituent particles and their relative content in the suspension. In this letter, we fully characterize the dependence of the composition on the microstructure and nanoscale dynamics in moderately concentrated, highly asymmetric colloidal suspensions of hard spheres in the liquid state. The large size mismatch between the constituent particles ($\kappa = 5$) results in an attractive interaction between the large particles arising from the depletion effect [12] and leads to the formation of monomodal domains. Using small angle

x-ray scattering (SAXS) and x-ray photon correlation spectroscopy (XPCS), we show that the multiple time scales observed for all the values of ε_B , correspond to motion of the particles within such domains. In particular, we find that the motion of the small particles is independent of composition while that of the large particles depends on the size of the large-particle-rich domains. We studied mixtures comprised of latex spheres of radii $R_B = 54$ nm and $R_S = 11$ nm dispersed in glycerol. The combined volume fraction of the particles was kept constant at $\phi = 0.4$. The impact of the composition on the microstructure and particle dynamics was addressed by studying a series of suspensions with a systematic variation in the relative content of the large spheres, $\varepsilon_B = 0, 0.04, 0.17, 0.28, 0.48, 0.68, 0.77, 1$. Measurements were performed at the beamline 8-ID-I at the Advanced Photon Source using coherent x-rays at 7.35 keV. The suspensions were sealed in glass capillaries and cooled using a LN2 flow cryostat. X-ray speckle patterns were collected with a CCD. Autocorrelations across the series of CCD frames were used to determine the intermediate structure factor:

$$F(q, \tau) = \exp(-(\tau/\tau_0(q))^{\beta(q)}), \quad (1)$$

where q is the wavevector, $\tau_0(q)$ is the characteristic time scale for structural relaxation and $\beta(q)$ is a measure of the $\tau_0(q)$ distribution within the measured $F(q, t)$. The SAXS profiles for different compositions, along with a typical speckle pattern, are shown in Fig. 1. The monomodal suspensions ($\varepsilon_B = 0$ and 1) data can be modeled using the hard-sphere model (HSM) with a nearest-neighbor separation distance of $R_{SS} = 28.2$ nm for $\varepsilon_B = 0$ and $R_{BB} = 126.8$ nm for $\varepsilon_B = 1$. The SAXS data of the mixtures show a transition between the monomodal limits with increasing ε_B that could not be described using the approach of a uniform mixture of hard spheres [13]. A high asymmetry ($\kappa \gg 1$) leads to a depletion effect [12], that results in a minimum energy configuration in which the large particles are in contact with each other. In the case of micron sized spheres with $\kappa = 5$, the separation of the particles into monomodal domains was directly observed using optical microscopy [7]. Based on this idea, a local monodisperse approximation (LMA) [14] was used to model the scattered intensity $I(q)$

$$I(q) \propto \phi_B S_{BB}(q) f_B(q) + \phi_S S_{SS}(q) f_S(q) + \phi_M f_M(q), \quad (2)$$

where ϕ_B and ϕ_S are determined by the volume fraction of the domains, $f_B(q)$, $f_S(q)$ are the form factors and $S_{BB}(q)$ and $S_{SS}(q)$ are the partial structure factors of larger and

smaller spheres, respectively. The minor contribution from the mixed term to the scattering intensity is described by a dilute suspension of ϕ_M spheroids with radius R_M and form factor $f_M(q)$. We found that $S_{SS}(q)$ is well approximated by the HSM. There is no agreement in the literature about the appropriate model for $S_{BB}(q)$ but the sticky hard sphere model (SHSM), with a square well attractive potential at a distance $R = 2R_B$ from the sphere center, is often argued to be more representative than the HSM [15, 16]. The nature of the inter-particle attraction is described by the depth, u_0 ($0 < u_0 < \infty$), and range, Δ of the attractive potential well, and enters the SHSM via the parameter Γ parameter [17], where:

$$\Gamma = \frac{12\Delta}{2R_B + \Delta} \exp(u_0/k_B T), \quad 0 < \Gamma < \infty \quad (3)$$

Our initial analysis yielded $\Delta = 6.8$ nm for all the bimodal suspensions. Since the fit was not sensitive to small changes about this value, it was kept fixed to minimize the number of free parameters. As shown in Fig.1, the LMA model reproduces all the features of the SAXS data remarkably well. The fitting results are summarized in Table I. For $\varepsilon_B = 0.04$, the arrangement of the large spheres was well described within the dilute suspension limit [$S_{BB}(q) = 1$]. When more large spheres were added ($\varepsilon_B \rightarrow 0.17$), the partial structure factor $S_{BB}(q)$ becomes more pronounced and Γ reaches a maximum value. We interpret this result as a signature of strong micro-phase separation driven by the depletion effect. Further increases in ε_B is accompanied by decreases in Γ that indicate a weakening of the attractive potential. R_{SS} was found to increase with increasing ε_B . This is in agreement with the simulations of the suspension with $\kappa=5$ and $\phi=0.4$ [8] where clustering of the larger spheres was observed, allowing more free volume for the smaller particles.

The $\tau_0(q)$ profiles are shown in Fig.2. Since temperature impacts the observed time scales but does not affect the ε_B dependence, we describe here only the data collected at 255 K and 235 K. The monomodal suspension shows a $\tau_0(q)$ response that is typical for concentrated colloidal suspensions, namely a well pronounced “de Gennes” narrowing effect [18]. At small q , the dynamics for all the bimodal compositions are much slower than for $\varepsilon_B = 1$. This effect is most pronounced for $\varepsilon_B = 0.04$ and $\varepsilon_B = 0.17$, which exhibit nearly the same Brownian $\tau_0(q)$. At lower temperatures, the $\tau_0(q)$ response for all the bimodal suspensions converge for $q > 0.08$ nm⁻¹, exhibiting two minima at $q_1=0.087$ nm⁻¹ and $q_2=0.14$ nm⁻¹ [Fig. 2(b)]. At q_1 , $\tau_0(q)$ for the bimodal compositions are comparable to the pure small spheres ($\varepsilon_B = 0$, [red stars in Fig. 2(b)]). Finally, a crossover in $\tau_0(q)$

is observed for the bimodal suspensions at the shortest measured length scales ($q > 0.15 \text{ nm}^{-1}$), whereby the particle dynamics is faster compared to the pure suspension of small spheres. The complexity of the dynamics in bimodal systems is also reflected by a non-trivial $\beta(q)$ profile [Fig.3(b)]. The particle dynamics at larger length scales exhibit a stretched exponential decay with $\beta \approx 0.9$ for $q < 0.05 \text{ nm}^{-1}$. For $q > 0.05 \text{ nm}^{-1}$, β decreases dramatically, exhibiting a minima at q_1 and increasing again at the largest measured q 's. We propose a physical picture of the depletion-induced demixing, whereby the microstructure of the bimodal suspensions is consists of monomodal domains. The structural heterogeneity is reflected by the distribution of the measured characteristic time scales τ_0 having two main components corresponding to dynamics within the two monomodal domains, $\tau_0^B(q)$ and $\tau_0^S(q)$. The time scale distribution, described by $\tau_0(q)$ and $\beta(q)$ in Eqn. 1, depends on the effective contribution of the monomodal domains to the scattered intensity, $\omega_B(q)\tau_0^B(q)$ and $\omega_S(q)\tau_0^S(q)$. The weights, $\omega_B(q)$ and $\omega_S(q)$, are determined by the number of particles of each type, their shape and dimensions (f_B, f_S) and their local microstructure (S_{BB}, S_{SS}). Large particles scatter mostly in the forward direction [region *I* in Fig. 3a]. In contrast, the scattered intensity from the smaller spheres is much weaker but is distributed uniformly over the measured q -range. As a consequence, the time scales observed at smaller q 's are dominated by τ_0^B , while τ_0^S dominates at the larger q 's [region *III* in Fig. 3(a)]. In the intermediate q -range (region *II*), the two time scales contribute at a comparable level, resulting in a complex shape of the $\tau_0(q)$ profile that exhibits the same beating pattern as $\omega_B(q)$, with minima at q_1 and q_2 [arrows in Fig.1, Fig.2(c) and Fig.3(a)]. The presence of multiple time scales in the system determines the shape of $F(q,t)$, described with the help of the exponent β . The exponent β is large in the q regions dominated by either τ_0^B or τ_0^S and shows a broad minimum at the q 's where both time scales contribute to $F(q,t)$ with similar magnitudes. To verify the correctness of our interpretation, $\tau_0(q)$ was modeled for $\varepsilon_B = 0.48$. The ratio of the time scales was set to $\tau_0^B(q)/\tau_0^S(q) \approx 9$, based on the $\tau_0(q)$ data measured for the monomodal suspensions. The first two terms from the SAXS model (Eqn. 1) were used as an estimate for $\omega_B(q)$ and $\omega_S(q)$. Although simplified to a large extent, the proposed model reproduces the measured data very well [solid line in Fig.3(c)]. Physically, the scenario described above can be understood as follows. Aggregates or microphase-separated regions, consisting of several large spheres, are formed. They can be approximated by a dilute collection of particles with a hydrodynamic radius $R_H \gg R_B$

(Fig. 4(a)). The aggregates themselves behave like Brownian particles. Once attached to the aggregate, the larger spheres are trapped and need to overcome the osmotic pressure exerted by the surrounding small particles to move freely again. In other words, a collective relaxation of the aggregate is required for the larger spheres to attain a new configuration thus explaining the significant slowing down of the larger length scale dynamics. This “adhesive” behavior explains the sticky nature of the larger spheres and is consistent with the SAXS results.

When more large spheres are added to the suspension, the clusters grow bigger yielding a measurable contribution to the scattering intensity from S_{BB} . For a given total volume fraction of the particles, the osmotic pressure exerted by the smaller particles is predicted to decrease with increasing ε_B [12] explaining the measured decrease in u_0 (decrease of the Γ parameter with increasing ε_B derived from SAXS). As illustrated schematically in Fig. 4(b), as the attractive interaction weakens, the dynamics within the large-particle-rich domains is less restricted and approaches the time scales observed for the $\varepsilon_B = 1$. The fact that the dispersion curves for all the bimodal suspensions converge for $q > 0.08 \text{ nm}^{-1}$ indicate that the growth of the larger sphere rich regions mostly influences the dynamics of the larger particles. At distances corresponding to the small sphere separation distances, the composition has negligible impact on $\tau_0(q)$. The proposed model is broadly applicable to bimodal suspensions exhibiting distinct time scales for particle dynamics as is typically the case in the phase-separation region of the phase diagram. For $\kappa > 6.46$, small spheres can fit between closely packed large spheres [19] yielding an extra component in the time scale distribution attributable to the dynamics of the small spheres confined between the large spheres. In the opposite limit, fluid and solid phases were reported to coexist even for $\kappa = 2$ [9]. Our model should be applicable to such low κ but we would expect a very complex $\tau_0(q)$ profile since both $\omega_s(q)$ and $\omega_B(q)$ would vary over the measured q range.

To summarize, we have presented a systematic study of the equilibrium dynamics in bimodal colloidal suspensions of hard spheres in the liquid phase. We show that spatial heterogeneity, until now observed only for colloidal gels, is also well pronounced in ergodic systems. Combined analysis of the static and the dynamic aspects of bimodal colloidal suspensions provides a comprehensive picture of the impact of the strength of the depletion forces on the microstructure and dynamics of the constituent particles. Our model successfully links the depletion effect and spatially heterogeneous dynamics. Similar to gels, the

level of dynamical heterogeneity is proportional to the strength of the attractive interaction between the large spheres which is controlled by their relative number concentrations in the suspension. The two main contributions to the distribution in time scales were attributed to the dynamics within the large- and the small-particle-rich domains. The depletion interaction is the strongest for small ε_B and the dynamics of the large spheres is restricted to a collective diffusion of the aggregates. As the attractive interaction weakens for $\varepsilon_B \rightarrow 1$, the large spheres move within the large immobilized aggregate on time scales approaching the values measured for the monomodal suspension while the time scales for the dynamics of the small spheres is constant.

We acknowledge S.-H. Lee and R. Ziegler for technical assistance. This work and the use of the APS are supported by the U.S. DOE, Office of Science, Office of Basic Energy Sciences, under contract No. DE-AC02-06CH11357.

TABLE I: Results from the SAXS micro-structural analysis.

ε_B	ϕ_B	ϕ_S	ϕ_M	R_M (nm)	Γ	R_{SS} (nm)
0.00	0.00	0.40	-	-	-	14.2
0.04	0.01	0.38	0.01	50.3	-	13.8
0.17	0.03	0.33	0.04	51.3	7.7	14.0
0.28	0.06	0.29	0.06	51.0	2.3	14.2
0.48	0.14	0.21	0.05	50.0	2.3	14.8
0.68	0.13	0.24	0.03	48.5	1.8	15.4
0.77	0.29	0.09	0.02	48.0	1.4	16.2
1.00	0.40	0.00	-	-	-	-

-
- [1] S.F.L. Watt *et al.*, *J. Geophys. Res.*, **114** B04207 (2009).
 - [2] L.B. Aberle *et al.*, *Macromol. Symp.* **162**, 249 (2000).
 - [3] G. A. Vliegthart *et al.*, *Europhys. Lett.* **62**, 600 (2003).
 - [4] P.B. Warren, *J. Phys. I France* **4** 237 (1994).
 - [5] X. Ye *et al.*, *Phys. Rev. E* **54**, 6500 (1996).

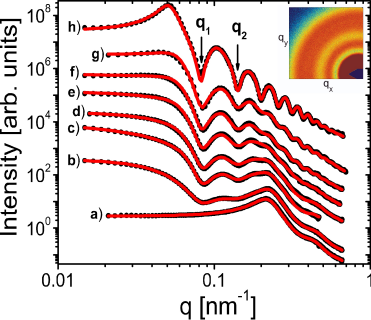
- [6] A. M. Kulkarni *et al.*, Phys. Rev. Lett. **83**, 4554 (1999).
- [7] S. Sanyal *et al.*, Europhys. Lett. **18**, 107 (1992).
- [8] M. Dijkstra *et al.*, Phys. Rev. E **59**, 5744 (1999).
- [9] A. D. Dinsmore *et al.*, Phys. Rev. E **52**, 4045 (1995).
- [10] S. R. Williams *et al.*, Phys. Rev. E. **64**, 041502 (2001).
- [11] J. M. Lynch *et al.*, Phys. Rev. E. **78**, 031410 (2008).
- [12] T. Biben *et al.*, Phys. Rev. Lett. **66**, 2215 (1991).
- [13] J. E. Enderby *et al.*, Physics and Chemistry of Liquids **1**, 1 (1968).
- [14] J. S. Pedersen, J. Appl. Cryst. **27**, 595 (1994).
- [15] D. Pontoni *et al.*, J. Chem. Phys., **119**, 6157 (2003).
- [16] R. Piazza *et al.*, Phys. Rev. E **58**, R2733 (1998).
- [17] S.V. G. Menon *et al.*, J. Chem. Phys., **95**, 9186 (1991).
- [18] P. Kleban, J. Stat. Phys. **11** 317 (1974).
- [19] R. K. McGeary, J American Ceramic Soc **44**, 513 (1961).

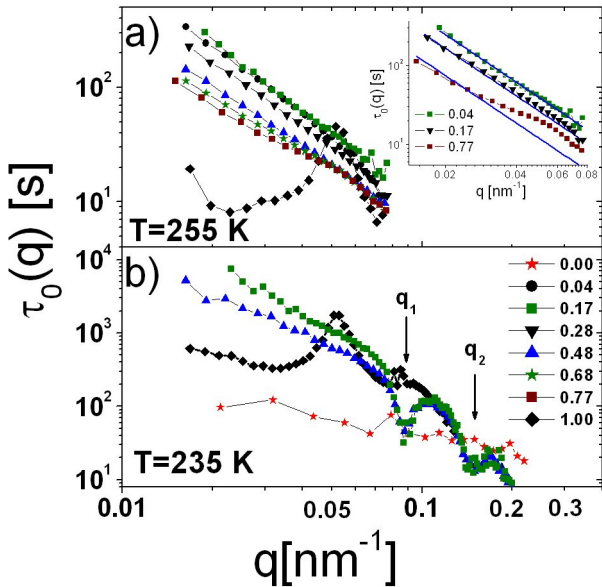
FIG. 1: SAXS profiles of bimodal colloidal suspension of latex spheres in glycerol. Curves are shifted vertically for clarity and arranged by the increasing content of large spheres from $\varepsilon_B = 0$ (a) to $\varepsilon_B = 1$ (h). Solid lines are the fits described in the text. Arrows indicate the positions of the first two minima, q_1 and q_2 , in the form factor for large spheres. The inset shows a typical speckle pattern corresponding to $\varepsilon_B = 0.48$.

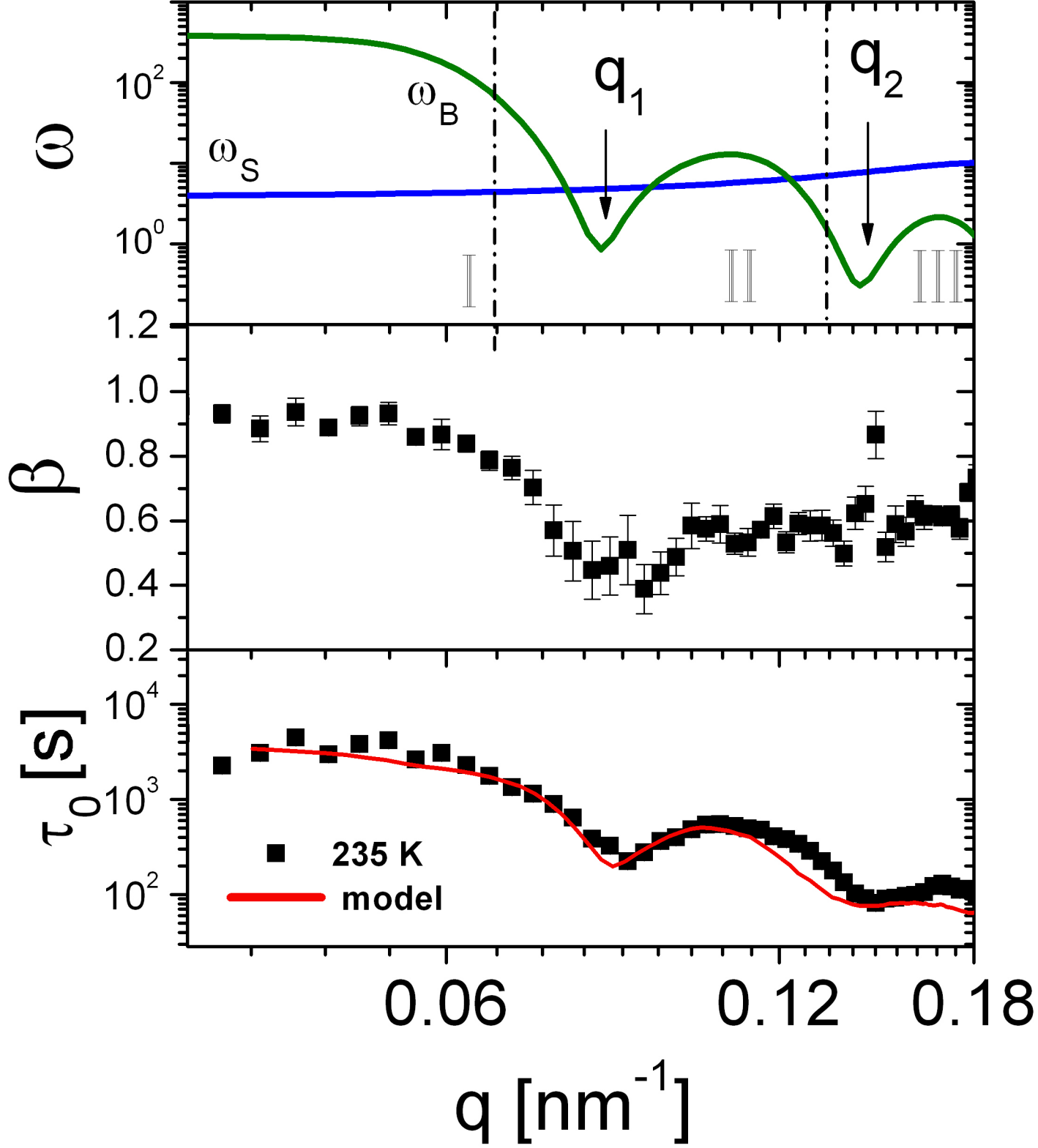
FIG. 2: Characteristic relaxation time scales for the bimodal colloidal suspensions at (a) 255 K and (b) 235 K. The inset shows $\tau_0(q)$ for $\varepsilon_B = 0.04, 0.17, 0.77$ with the dashed line showing the power-law dependence expected for Brownian motion.

FIG. 3: (a) $\omega_B(q)$ and $\omega_S(q)$ obtained from the the analysis of SAXS data for the $\varepsilon_B = 0.48$ suspension. The broken lines mark regions of q that are sensitive to the dynamics of: (I) large spheres, (II) large and small spheres, and (III) mainly small spheres. (b) Stretching exponent $\beta(q)$ and (c) relaxation time $\tau_0(q)$ extracted for $\varepsilon_B = 0.48$ at 235 K. The solid line in (c) represents the $\tau_0(q)$ modeled according to Eqn. 1.

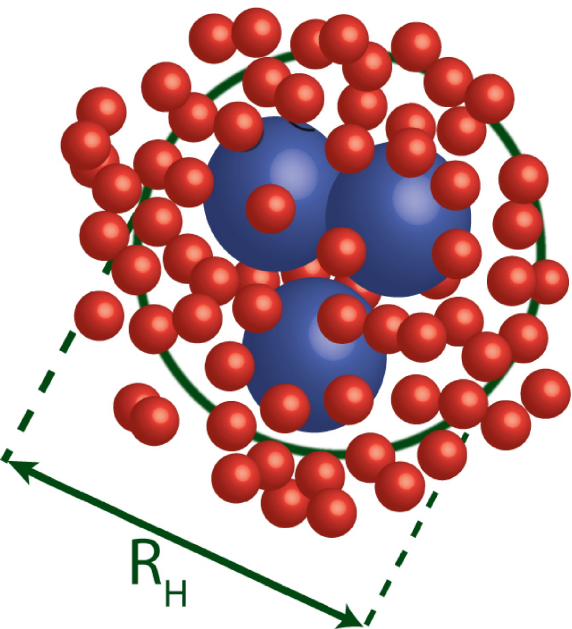
FIG. 4: Proposed physical picture for the large-sphere-rich aggregates for (a) low ϕ_B and (b) high ϕ_B . The effective hydrodynamic radius of an aggregate R_H is marked with a solid line in (a). The arrow indicates a possible rearrangement within the large sphere rich domain.







a)



b)

